# TMI-2 Transfer System
# Criticality Technical Report

Document No. 77-1155739-02

Published June 19, 1985

Babcock & Wilcox Company
Nuclear Power Division
Lynchburg, Virginia

Prepared for
GPU Nuclear Corporation
Under Master Services Contract 665-3212

TMI-2 Transfer System
Criticality Technical Report

Prepared by: P.L. Holman — 6/19/85
P. L. Holman, Principal Engr., B&W — Date

Approved by: W.G. Pettus — 6-19-85
W. G. Pettus, Advisory Engineer, B&W — Date

Approved by: P.C. Childress — 6-19-85
P. C. Childress, Project Manager, B&W — Date

CONTENTS

## LIST OF TABLES



## LIST OF FIGURES

## 1. Abstract

The TMI-2 defueling canisters will be transferred to locations within the reactor and fuel handling buildings using a transfer shield containing lead. Transfer of canisters to the shipping cask will utilize a different device called a transfer cask. This report examines K-effective for both the transfer shield and cask, with dimensions supplied by GPUN. The enclosed results indicate that for ruptured and non-ruptured canisters no poison materials other than those contained in the canisters are required in the design of either the transfer shield or cask to maintain K-effective <.95. Canisters with extensive internal damage and/or external damage from being dropped or deformed are not addressed since these canisters will be handled by GPUN on a case by case basis and are therefore not included in the current workscope. (2)

## 2. Introduction

Transfer of the Fuel, Filter, and Knockout canister designs within the reactor and fuel handling buildings is accomplished in part using the transfer shield and transfer cask. The function of the transfer shield is to allow safe removal and transfer of canisters out of containment for reactor defueling. The transfer shield will facilitate loading the canisters into the transfer basket for movement to the fuel handling building. A second transfer shield will be located within the fuel handling facility for the placement of canisters within the storage racks, subsequent transfer to a dewatering station, and transfer of canisters to a transfer cask loading station. A transfer cask will be located within the fuel handling building to allow movement of debris filled canisters into shipping casks. (2)

From the description provided in Reference 1 by GPUN the transfer shield comprises a long hollow cylindrical lead shield. The inside and outside of the lead shield will be lined with steel for structural support. A smaller movable outer lead shield will be lowered at least one foot below the water surface prior to withdrawal of the canister into the transfer shield. This outer shield can be raised once the canister is fully inserted to allow clearance of the shield from obstructions. The shorter length outer shields will also be lined with steel for structural support. The transfer shield will be attached to a canister handling trolly to allow transfer of the canisters within the shield as a unit. The canisters will be withdrawn into the transfer shield by a canister grapple and cables connected to a hoist which is mounted on the movable trolly. (2)

The transfer cask is similar to the transfer shield with the main walls of the transfer cask containing 4.5 inches of lead with 1 inch inner and outer

steel linings for structural support. The transfer cask has a movable bottom door to allow insertion of a canister by a grapple and cable mechanism and subsequent closure of the cask upon canister insertion. Located below the bottom door is a lead/steel-lined flange that projects outward from the cask to reduce levels of backscattered radiation. The hoist for the transfer cask is located to one side of the cask and near the cask midplane. The entire transfer cask is suspended by a crane. (2)

## 3. Transfer Shield and Cask Criticality Analysis

### 3.1. Background

The criticality studies in this report have proceeded at times in parallel or in advance of normally required mechanical design information. Where specific dimensions on the transfer cask or shield were available they were incorporated into the analysis. In some cases information was not available and dimensions were chosen in a fashion to produce a bounding analysis and maintain conservatism. For further details see the section on assumptions.

Calculations in this report address the following objectives: (1) evaluate the optimal fuel composition with the lead shield in place, (2) determine the effect of the gap region between the inserted canister and the cask or shield for centered and off-centered canisters, (3) determine the most reactive canister type in the transfer shield, (4) evaluate the most reactive insertion point for a canister in the transfer shield, and (5) evaluate the most reactive canister for the worst insertion point in the transfer cask. Canister criticality results for both ruptured and non-ruptured as well as single and lattice configurations are summarized in recent technical reports.[2,3] (2)

### 3.2. Scope of Calculations

The required scope of criticality calculations is detailed in the "Technical Specifications for Design of Defueling Canisters for GPU Nuclear Corporation Three Mile Island Unit 2 - Nuclear Power Plant" Appendix E, Section 1.2.[4] Section 1.2.3 specifically details transfer criticality, although subsequent changes to the work scope were negotiated. (2)

### 3.3. Reactivity Criterion

The reactivity criterion for criticality safety used in this analysis is that the value of K-effective for the most reactive canister inside the

transfer system shall not exceed 0.95. These analysis are consistent with 10CFR72.73 and ANSI/ANS 8.1, 8.17, and 16.5[5,6,7,8] within the workscope negotiated by GPUN. (2)

3.4. Calculational Assumptions

The calculational models for the canisters[2,3] in the transfer shield or cask assume the following conservative conditions:

1. Batch 3 unirradiated fresh fuel only.
2. Enrichment: batch 3 average + 2σ (2.98 wt% U235).
3. No cladding or core structural material.
4. No soluble poison or control materials from the reactor core.
5. Optimal fuel lump size and volume fraction and optimal water moderator density (except in parametric cases for the optimization study).
6. Canister fuel regions completely filled without weight restriction. If a weight restriction were to apply and canisters were partially filled with clean water or structure the result would be lower canister reactivity.[3] (2)
7. At least 2σ allowance in fixed poison concentrations.
8. Uniform 50°F temperature.
9. Infinite media Dancoff factors (see Dancoff Factor Assumptions).

The model for the transfer shield assumes the following conditions (See Figure 1 for revision 1 model and Figure 2 for revision 2 model).

I. The trolly was modeled as a 4x4 foot, 12 inch thick block of steel. This assumption will be conservative since steel in air will be a good reflector of epithermal neutrons.

2. A movable horizontal lead shield 15.5 inches in diameter is assumed to be 6 inches thick and located 20 inches from the top of the upper canister head at all canister insertion levels. Because of the conservative size of this lead shield, the grapple was not specifically modeled.

3. The shield walls were originally assumed to be made entirely of lead for the transfer shield to provide maximum reflection without absorption or removal of epithermal neutrons. This assumption applies to all transfer shield cases originally contained in revision 1 of this document. For revision 2 calculations the steel liners are explicitly modeled. (2)

4. For revision 1 calculations the lead walls were assumed to be 5.125 inches thick which includes the 0.125 inch air gap modeled as being lead filled for conservatism. Additionally, the inside diameter of the walls are 15.5 inches and extend the entire length of the transfer shield. Revision 2 analyses assume an inner shield wall that extends the full length of the transfer shield with a combined steel and lead thickness of 3-7/32 inches. The inner full length shield is followed by an 11/64 inch air gap and a 9 ft long movable outer shield. The 9 ft long movable outer shield has a combined lead and steel thickness of 2-5/32 inches. Attached to the movable outer 9 ft shield is a shorter 30 inch long shield with a lead and steel thickness of 2-61/64 inches. These dimensions yield a maximum lead and steel thickness less the air gap of 8-21/64 inches at the base and a minimum thickness of 3-7/32 inches above the 9 foot long outer shield. The inside diameter of the transfer shield is 15-5/8 inches. Shown in figure 3 is a cross-sectional cut of the transfer shield wall with lead and steel dimensions. (2)

5. For revision 1 calculations the water level of the pool is level with the bottom of the transfer shield since lead with an air gap between the canister and shield was shown to be more reactive than lead with a water gap (see canister shield gap analysis). In revision 2 analyses the canister-shield gap was air filled as before but water was modeled for a length of 2 feet outside the shield to maximize reflected neutrons to the canister. This modification was shown with XSDRNPM to be conservative (2)

(see section 3.10 - transfer shield water reflector analysis).

6. Dry air is modeled in the region between the canister and shield and in regions external to the shield. This will minimize thermalization of reflected neutrons and reduce subsequent absorption in non-fissioning structural material. Dry air is assumed to consist of pure oxygen and is conservative since it has both a smaller removal and absorption cross-section than nitrogen. Assuming air to consist of pure oxygen will have a negligible effect on K-effective considering the small density of air even for the 20 inch vertical gap between the top of the canister and lead shield. There are three orders of magnitude difference between the density of air and a material like water. Furthermore results of the canister shield gap analysis (see Section 3.9.2) shows a trend that indicates the most reactive material for the gap region that could be assumed is void. Finally, since the top and bottom heads of the canister are low importance and low fission density regions the effect of the assumed composition of air in this region is insignificant on calculated results with a probabilistic code like KENOIV. (2)
7. Although there is an air gap between the bottom of the transfer shield and the water level when the outer shield is raised, this gap is not modeled to prevent neutron streaming.
8. No soluble boron is assumed in any water regions.
9. For the canister types examined, only internally ruptured configurations due to filter screen failure were examined in the transfer shield since these are most reactive.[2,3] (2)
10. The upper head protective skirt on the canisters is not modeled.

11. The transfer shield in revision 2 calculations models the latest knockout canister geometry with shorter $B_4C$ rods. (2)

The model for the transfer cask assumes the following (see Figure 4):

1. No trolly is modeled since the transfer cask is supported by a crane (2)
2. A horizontal lead shield 15 inches in diameter is assumed to be 6 inches thick and located 10 inches from the top of the upper canister head. Because of the conservative size of this lead shield the grapple was not specifically modeled.
3. The 15 foot 1 inch long upper lead shield is assumed to have 4.5 inches of lead with a 1 inch steel liner on all sides. The inside diameter of the main shield is 15 inches.
4. The bottom lead door is assumed to be 4 inches thick with 0.5 inches of steel liner on all sides. The diameter of the bottom door is conservatively extended to 43 inches in revision 2 analyses. (2)
5. The lead/steel flange located below the bottom door projects 7.5 inches radially beyond the main cask walls. This flange is 4 inches thick with a 0.5 inch liner on all sides. The radial width of the flange is 14 inches.
6. The region below the 4 inch thick lead-door was filled with lead for conservatism in revision 2 calculations. This gives a combined lead and steel thickness below the canister of 10 inches. (2)
7. A lower shield collar (loading boot) is assumed to be 3 feet long, with a thickness of 3 inches of lead and 1 inch of steel liner on all sides. Although the loading boot is no longer required it is retained for conservatism. (2)

Figure 1

Revision 1 Transfer Shield Model

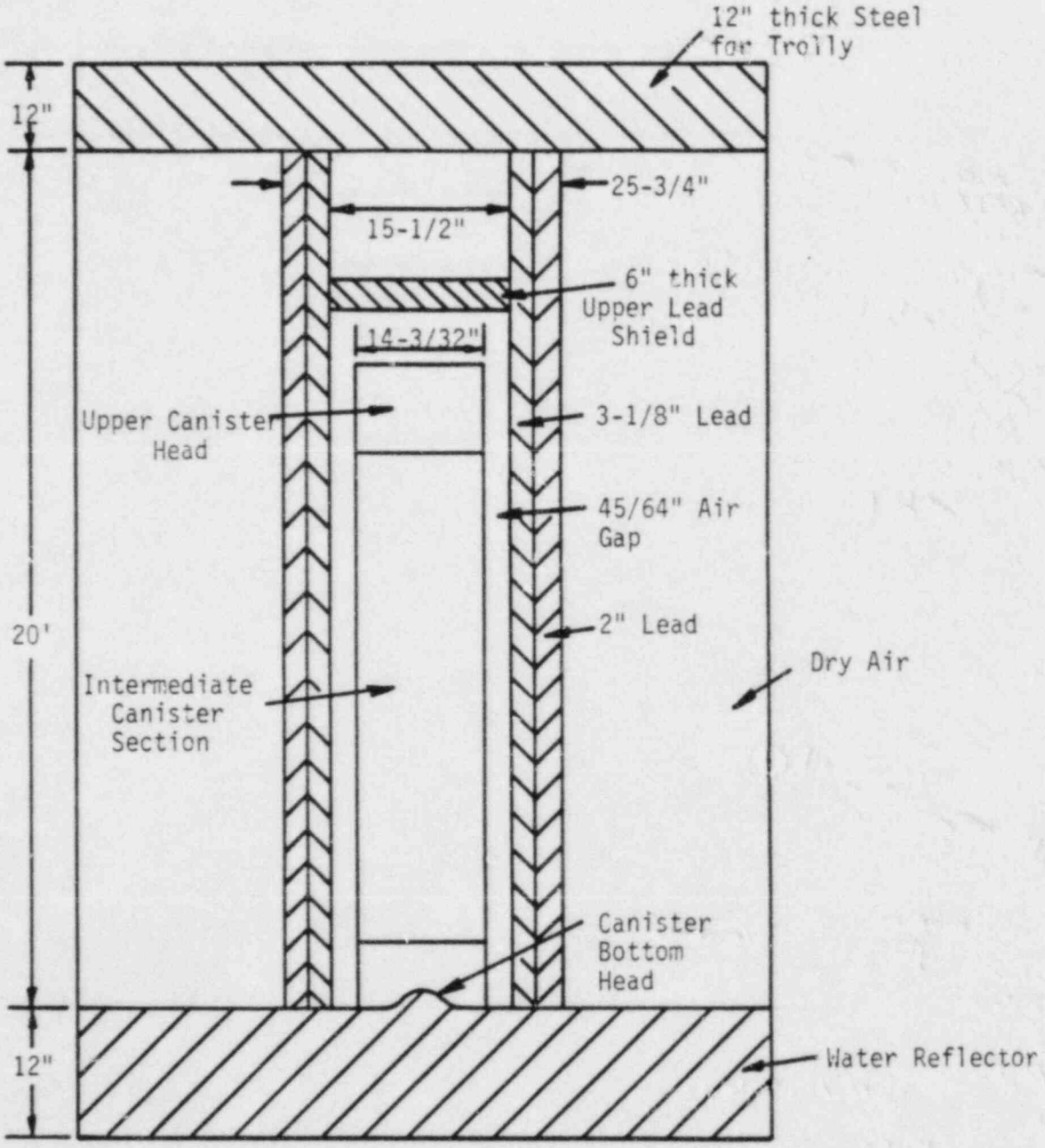

Figure 2

Revision 2 Transfer Shield Model

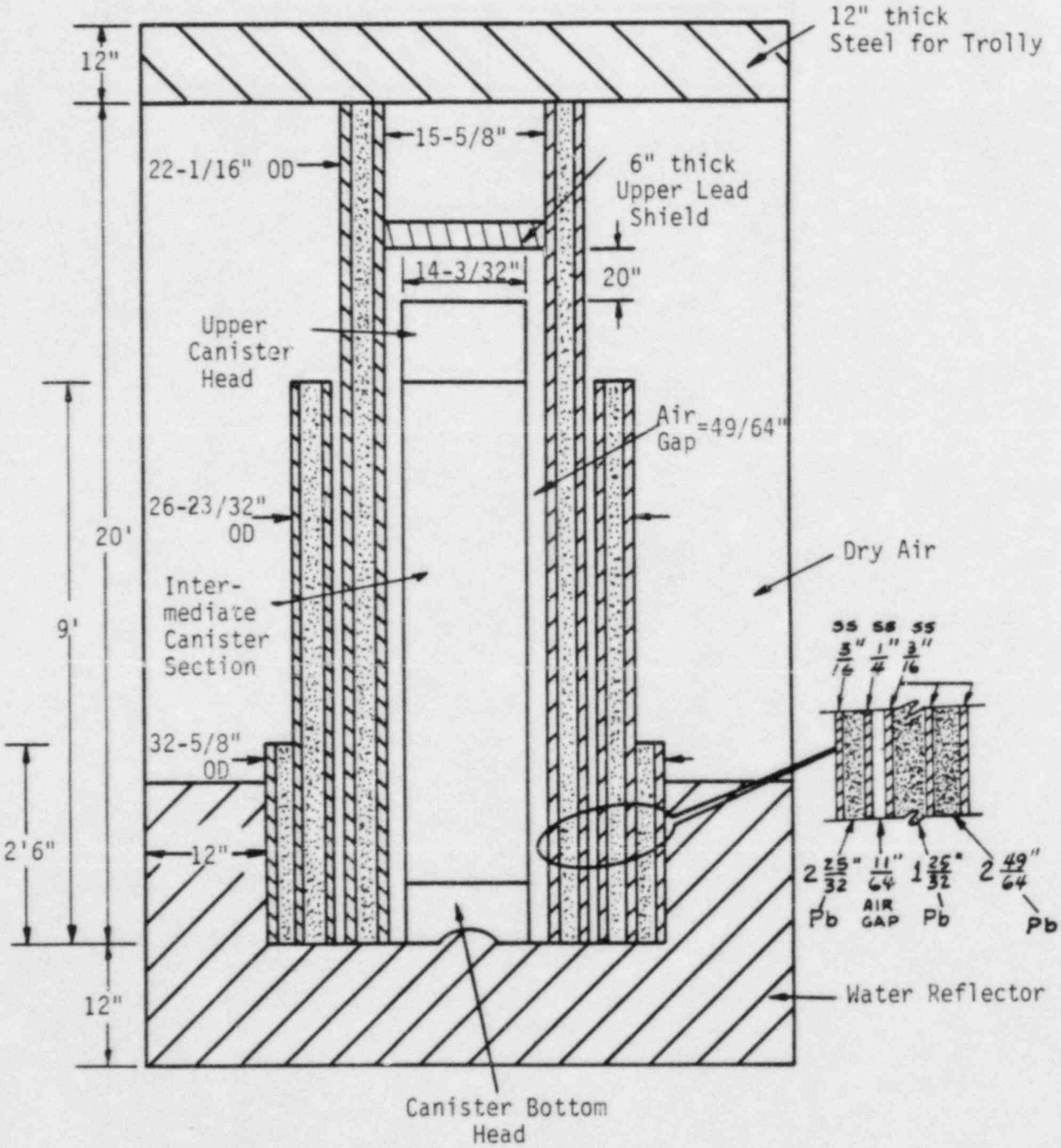

Figure 3

Transfer Shield Wall Cross-Section

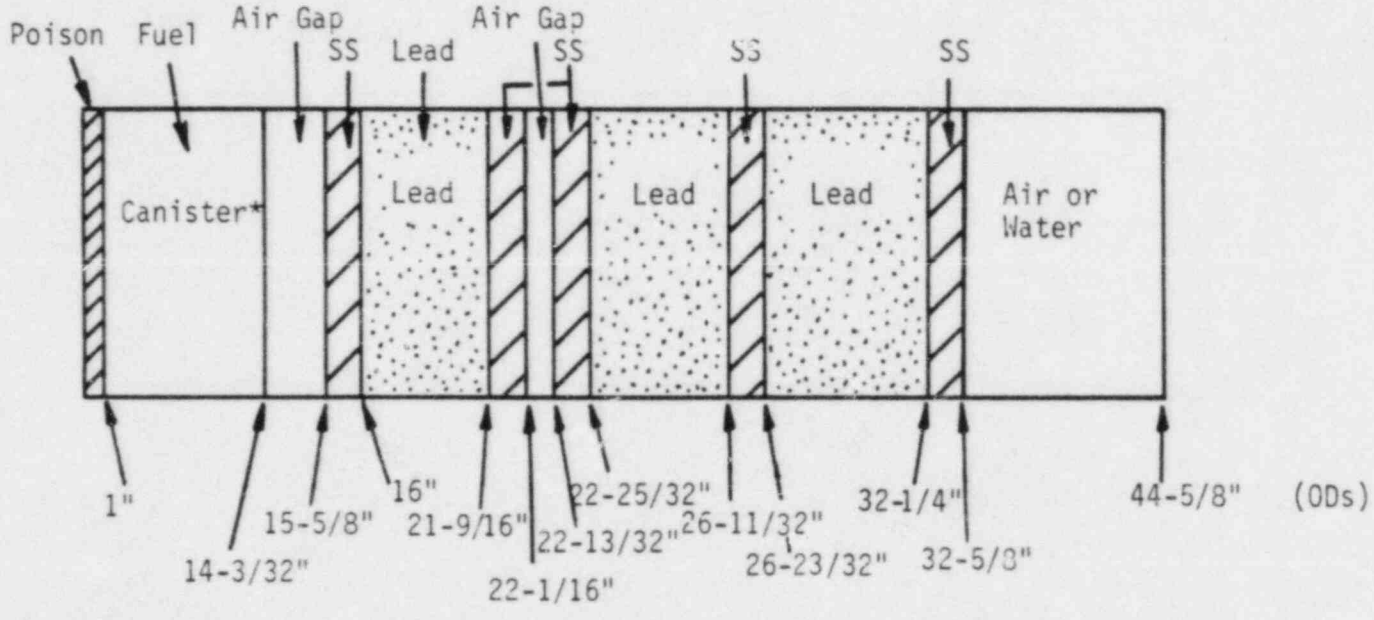


*All knockout canister detail not shown.

Figure 4

Transfer Cask Model

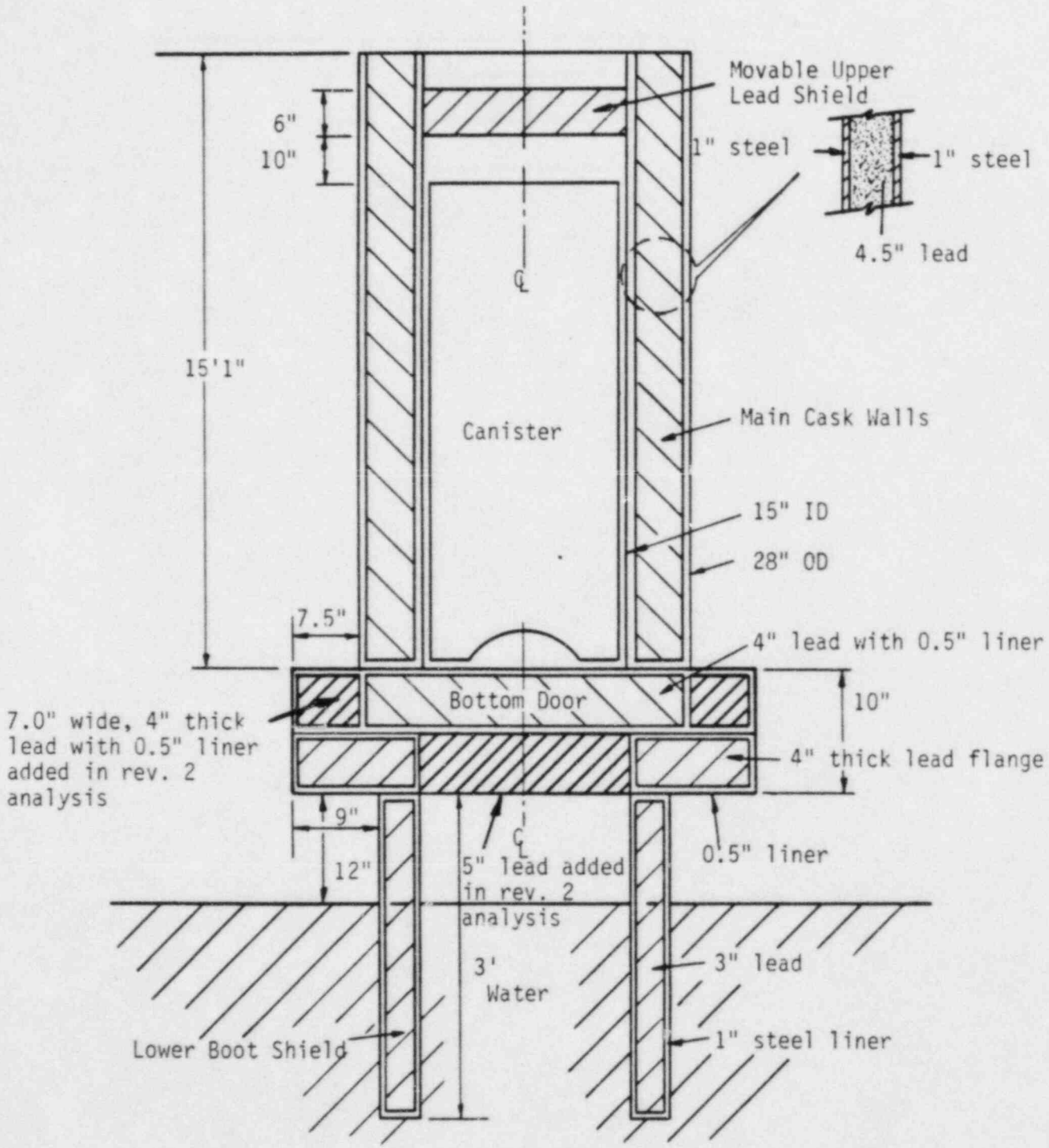

8. The loading boot extends 2 feet below the water surface.
9. Dry air is modeled in the gap region between the canister and cask and in regions above the water surface external to the cask.
10. No soluble boron is assumed in any water regions.
11. Only internally ruptured canister configurations due to screen failure were considered since these are most reactive.[3] (2)
12. The protective skirt on the canisters are not modeled.
13. The transfer cask models the knockout canister with the latest geometry and shorter $B_4C$ rods in revision 2 analyses. (2)

3.5. Dancoff Factor Assumptions

An obvious limitation in generating cross-sections for complicated geometrical configurations where differing fuel regions are involved is determining the effective Dancoff self-shielding effect on epithermal fuel resonances. The Dancoff factor using Sauer's method can be analytically determined for only the simplest geometries. In the case of the three canister designs, the fuel region geometries cannot be treated analytically with respect to Dancoff factors. In this analysis it is only necessary to demonstrate that whatever Dancoff factors are utilized they result in the prediction of a conservative eigenvalue. For this purpose, the NULIF code was utilized. Evaluation of NULIF results with different Dancoff factors indicates that any increase in the Dancoff D=(1-C) factor from the infinite cell array condition results in a decrease in K-effective as a result of decreased U238 self-shielding. Results also indicate that the potential decrease in K-effective is greater for higher density fuel. In the determination of Dancoff factors for cross-section sets used by KENOIV and XSDRNPM, infinite cell array conditions will be assumed for conservatism.

### 3.6. Computer Codes and Cross Sections

The computer codes used in this work were NULIF[9], NITAWL[10], XSDRNPM[11], and KENOIV[12]. The NULIF code was used only for the study of Dancoff factor effects. NITAWL and XSDRNPM were used for processing cross-sections from the 123 group AMPX master cross-section library.[13] NITAWL provides the resonance treatment and formats the cross-sections for use by either XSDRNPM or KENOIV. In all cases XSDRNPM cell weighted cross-sections are used by KENOIV and XSDRNPM/ANISN type calculations.

### 3.7. KENOIV Bias

No benchmark results are included in the current workscope to allow a direct assessment of the KENOIV bias for a fuel/lead system. However, the comparison of results between critical experiments and KENOIV[14,15] indicates a trend of increasing KENOIV bias related only to the spacing between fuel assemblies with no discernable trend due to materials placed between assemblies. The materials placed between the assemblies were stainless steel, aluminum, and $B_4C$ rods, they provide a sufficient density change to indicate if there is a related bias. Since none is obvious, it is assumed that a significant trend does not exist. This assumption is carried over for the single canister, where it is assumed that the KENOIV bias is not dependent upon the reflector density. Thus, the bias for this case is assumed to be that of the single canister in water. i.e. 0.02$\Delta$k.[3] (2)

### 3.8. Fuel Optimization for Lead Shielded Canisters

#### 3.8.1. Background Information and Assumptions

Of interest in this extension of the fuel optimization study is the effect of the external lead shield which makes up the transfer shield and transfer cask. To examine the effect of the lead shield on the optimized fuel mixture, simplified KENOIV and XSDRNPM models were utilized. Assumptions used

in this optimization study which were based on previous canister studies contained in references 2 and 3.

3.8.2. Fuel Optimization Results

It was decided to benchmark KENOIV against XSDRNPM for simple cell types and to use XSDRNPM to quantify the effect of the lead shield. A simple 2D cell was run with KENOIV which consisted of a 14 inch diameter fuel region surrounded by water. No poison rods are modeled for these simple cases. This case was run for .31 and .37 volume fraction cases and when taken with the infinite media NULIF results[2,3] predict the .31084 fuel volume fraction to be optimum. These results are shown in Table 1. Two XSDRNPM cases were run for a 13.5 inch diameter fuel region with a 1/4 inch thick steel outer shell surrounded by water. These XSDRNPM results also indicate the .31084 volume fraction is optimum and are shown in Table 1.

A six inch lead shield was modeled around the outside of the 14 inch canister in XSDRNPM. The lead shield had a 15.5 inch inside diameter resulting in a .75 inch dry air gap between the canister and the lead shield. Dry air was also modeled outside the six inch thick lead shield. Six inches of lead was chosen since it was considered to be the maximum thickness of lead for either the transfer shield or transfer cask. No modeling of the steel liners on the shielding was considered. Dry air was also considered to consist of pure oxygen.

Three lead shielded XSDRNPM cases were performed for volume fractions of .25, .31084, and .37. The resulting eigenvalues are shown in Table 1 and demonstrates for the lead shield cases that the optimum fuel volume fraction remains as .31084. For the .31084 fuel volume fraction a six inch lead shield causes a .055 increase in delta K-effective over the water moderated case.

This is the result of both decreased absorption in hydrogen and the canister shell as well as epithermal back-scattering of neutrons from the lead to the canister.

One final case was performed with XSDRNPM to determine the effect of a decrease in the water density for the fuel-water mixture in the canister surrounded by lead. New NITAWL-XSDRNPM cross-sections were generated for the .31084 fuel volume fraction with a 95% nominal water density. The result was a decrease in K-effective of .015$\Delta$k due to the decreased hydrogen density and neutron thermalization.

Table 1. Comparison of KENOIV and XSDRNPM Results for Simple Cell Types With and Without Lead and No Poison Rods*

| Cell Type | Model | Vol. Fraction | K-effective/2$\sigma$ dev. | Neutron Histories | |
|---|---|---|---|---|---|
| 14 inch dia. fuel, no steel, w/$H_2O$ | KENOIV | .31084 | 1.07±.010 | 18963 | (1) |
| " | KENOIV | .37 | 1.065±.008 | 19565 | (1) |
| 13.5 inch dia. fuel, 1/4 in. steel can, w/$H_2O$ | XSDRNPM | .31084 | 1.0300 | - | (1) |
| " | XSDRNPM | .37 | 1.0195 | - | (1) |
| 13.5 inch dia. fuel, 1/4 in. steel can, w/air gap and 6 inch lead shell | XSDRNPM | .25 | 1.0797 | - | (1) |
| " | XSDRNPM | .31084 | 1.0853 | - | (1) |
| " | XSDRNPM | .37 | 1.0712 | - | (1) |
| (95% Nominal $H_2O$ Dens.) | XSDRNPM | .31084/95% $H_2O$ | 1.0703 | - | (1) |

*The absolute magnitude of K-effective is not significant. Simple cell results are only used to indicate trends.

## 3.9. Canister-Shield Gap Criticality Analysis

### 3.9.1. Model Description and Background

When the transfer shield is lowered into the pool to allow insertion of a canister, part of the gap region between the transfer shield and canister will be water filled and part of it may contain only air. To determine the most critical canister configuration in the shield it is necessary to quantify the effect of the .75 inch gap region. For this analysis XSDRNPM was used since the changes in reactivity due to the gap are small and would not be suited for a Monte-Carlo code with its associated uncertainties. Two additional XSDRNPM cases were run for the optimal fuel volume fraction of .31084 with 50°F nominal density water and 5% dense water in the gap region. The lead shield was assumed to be six inches thick and the canister was modeled as a 13.5 inch diameter fuel region with a 1/4 inch steel shell. No poison rods are modeled in these simple canister types.

### 3.9.2. Gap Analysis Results

The results shown in Table 2, which include two cases from the fuel optimization study, demonstrate that the most reactive configuration occurs with an air gap between the lead shield and canister. These results are explained by the backscatter of neutrons from the lead shield to the water filled canister. The air between the canister and shield attenuates few neutrons and does not contribute significantly to the thermal neutron spectrum. Without the consideration of 3D geometry induced leakage effects these results predict the most critical configuration for a canister is to be fully inserted into the transfer shield.

Table 2. XSDRNPM K-effective Results For Canister-Shield Gap Analysis*

| Model Description | K-effective | |
|---|---|---|
| Fuel Canister (14 in. dia.) and water only | 1.030 | (1) |
| Fuel Canister (13.5 in. dia. fuel, 1/4 inch steel shell, .75 inch water gap, 6 inches lead) | 1.066 | (1) |
| Fuel Canister (13.5 in. dia. fuel, 1/4 inch steel shell, .75 in. 5% water density gap, 6 inches lead) | 1.0848 | (1) |
| Fuel Canister (13.5 in. dia. fuel, 1/4 inch steel shell, .75 in air gap, 6 inches lead) | 1.0853 | (1) |

*The absolute magnitude of K-effective is not significant. Simple cell results are only used to indicate trends.

## 3.10. Transfer Shield Water Reflector Analysis

### 3.10.1 Model Description and Background

Revision 1 analysis did not have water modeled on the outside of the transfer shield because when the canister is fully inserted into the shield it is above the water level. This was determined to be the most reactive insertion point (see section 3.13. Canister Insertion Analysis.) Additionally, the XSDRNPM gap analysis (section 3.9) demonstrated that an air or void filled gap is most reactive. In the subsequent revision 2 analyses that incorporate the latest knockout canister geometry it was theorized that a 2 foot high water reflector outside the shield may help reflect neutrons back to canister and prove to be an additional conservative modeling assumption. Therefore in revision 2 transfer shield analyses, the following conservatisms will be implemented. (2)

1. The outer movable shield will be completely raised to maximize the total lead and steel thickness,
2. The water level of the pool will be raised to a height 2 feet from the bottom of the transfer shield to help reduce leakage,

3. The canister-shield gap region will be assumed to consist entirely of air to maximize reactivity of the system, and
4. Water will be assumed along the bottom of the canister to reduce leakage and prevent neutron streaming (compare Figures 1 and 2).

### 3.10.2. Water Reflector Results

Two cylindrical XSDRNPM cases were performed modeling a canister with a centeral poison rod surrounded by the transfer shield geometry according to Figure 3. One case was run with a 1 foot wide air reflector and one with a 1 foot water reflector. In both cases the canister shield gap region was filled with air to be consistent with the conservative manner in which later 3D KENOIV transfer shield cases would be run. The results of this analysis, shown in Table 3 demonstrate that the water reflector external to the lead shield is a positive reactive addition by reducing neutron leakage. The difference in K-effective for these two cases is $\sim$.0081$\Delta$k. The 2 foot (2)
increase in water level above the canister bottom in the external region around the shield comprises only 16.4% of the knockout canister length. Since the XSDRNPM calculation is modeling the water region over the entire length of the shield the reactivity increase in the 3D KENOIV model is much less than .0081$\Delta$k. It is also important to recognize that the bottom canister region has less neutron importance than the middle regions of the canister. For simplicity, if we assume all canister regions are equally important, it is expected that the increase in K-effective of this already conservative model would be approximately .0013$\Delta$k.

For the early revision 1 analysis this increase in K-effective from the 2 foot water level is more than offset by the extension of the outer lead shield the full length of transfer device. Additionally, if the entire canister

shield gap region contained water instead of air, K-effective based on XSDRNPM results would drop by approximately .0193Δk (see section 3.9.) Therefore the gap region between the canister and shield appears to be worth more in terms of reactivity than the water or air region surrounding the lead transfer shield. For these reasons the calculated K-effectives from the revision 1 transfer system analysis are conservative. Although it is recognized that it is physically impossible to have an air gap between the canister and shield and have water outside the shield at the same level, this change was implemented in all revision 2 transfer shield analyses. (2)

Table 3. XSDRNPM Water Reflector Analysis*

| Model Description | K-effective | |
|---|---|---|
| Canister in steel and lead shield, air gap, and air reflector | 1.02742 | (2) |
| Canister in steel and lead shield, air gap, and water reflector | 1.03548 | (2) |

*The absolute magnitude of K-effective is not significant. XSDRNPM results are only used to indicate trends.

## 3.11. Off-Centered Canister in Transfer Shield

### 3.11.1. Model Description and Background

To assess the effect of a canister that is off-center in the transfer shield or swinging from side-to-side within the shield, the XSDRNPM code was utilized. The off-centered canister was modeled inside the shield using 1D slab geometry with a buckling factor to allow axial leakage. The entire diameter of the shield was modeled plus 1 foot of air on either side. The gap region was assumed to contain air. Shown in Figure 5 is the geometry detail of the off-centered canister case. The thickest lead region of the transfer shield was modeled since this would maximize the number of reflected neutrons (2)

Figure 5

Off-Centered Canister XSDRNPM Model

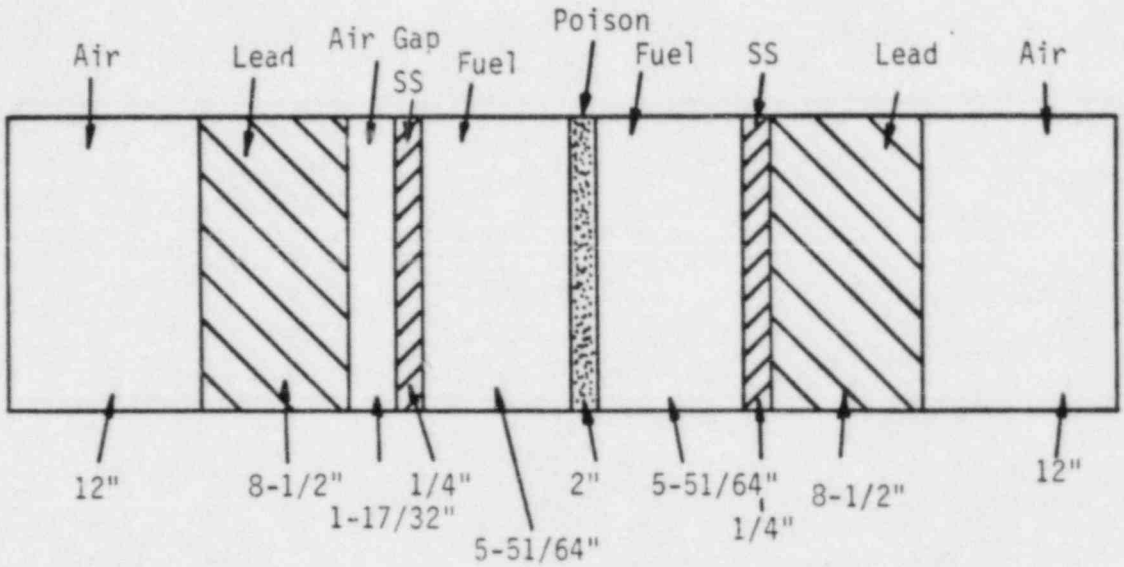

to the canister. The two inch poison rod in the center of the canister was also modeled.

3.11.2. Off-Centered Canister Results

The results for centered and off-centered canister XSDRNPM calculations are shown in Table 4. For the centered canister case the gap modeled is 49/64 inches on either side of the canister. For the off-centered case, the total gap width of 1-17/32 inches is modeled entirely on one side of the canister with the other side flush against the steel-lined lead wall. Examination of the results of these two cases indicate that the difference in K-effective is ~.0001Δk which is considered negligible. Additionally, the centered canister is most reactive. Therefore, for the remainder of this analysis all canisters will be assumed to be centered within the respective shields. (2)

Table 4. XSDRNPM K-Effective Results For Off-Centered Canister*

| Model Description | K-effective |
|---|---|
| Centered Fuel Canister | 1.05547 |
| Off-Centered Fuel Canister | 1.05534 |

*The absolute magnitude of K-effective is not significant. Simple cell results are only used to indicate trends.

3.12. Canister Optimization in Transfer Shield

3.12.1. Model Description and Background

For determining which canister type is most reactive in the transfer shield and the similar transfer cask, a 3D KENOIV transfer shield model was used. For conservatism in revision 1 analyses the 9 foot long outer shield was extended the full length of the transfer shield. In a similar manner the 16 foot long inner shield was extended to the water level. The steel inner (2)

and outer liners on each shield and the air gap were modeled as lead giving a combined thickness of 5.125 inches. A circular shaped 3 inch lead plate is located 20 inches above the top of the canister. A smaller 3 inch lead shield is located within the canister grapple. These two shields were combined to form one 6 inch lead shield 20 inches above the canister. Although few neutrons will penetrate the 6 inch circular shield, the rest of the transfer shield was modeled by an additional 7.84 feet of shielding with a 1 foot thick block of steel placed horizontally on top of the shield to represent the trolly underframe. The total length of the thickened lead shield and trolly underframe is 21 feet. This structure is surrounded by 1 foot of water (up to the bottom of the shield) on all sides. The transfer shield was not extended below the water surface in the original analyses since it was shown by previous XSDRNPM calculations in Table 2 that the lead shield with an air gap is most reactive. The water level was also extended to the bottom of the canister and shield to preclude neutron streaming out of the transfer shield when the outer shield is raised. The previously described transfer shield model is shown in Figure 1. (2)

The ruptured knockout and filter canisters were modeled in 3D with this transfer shield model to determine which canister type is most reactive. The fuel assembly canister was not considered since concrete will be placed in the outer lobes and will prevent the more reactive ruptured configuration. For canisters with this concrete modification in a 17.3 inch array, K-effective is $0.829 \pm 0.025$[3]. This K-effective is low enough relative to the knockout canister 17.3 inch lattice K-effective[3] that the fuel canister can be eliminated from consideration. (2)

### 3.12.2. Transfer Shield Optimization Results

The results of the transfer shield analysis with the ruptured knockout and filter canister fully inserted into the shield demonstrate the knockout canister to be most reactive. These results are shown in Table 5 and indicate that the ruptured knockout canister is .036±.014Δk more reactive than the ruptured filter canister in the transfer shield. The respective increase in K-effective from the lead shield for the knockout and filter canister cases is .043±.018 and .045±.018. It should be recognized that the no shield cases in Table 5 were taken from Reference 2, and have an overly high K-effective from the previously documented U238 cross-section treatment. If the .015Δk conservatism[3] is subtracted from these results the increase in K-effective from the 5.125 inch lead shield becomes .058±.018 and .060±.018, respectively for the two cases examined. This increase in reactivity is in good agreement with the .055Δk reactivity increase from XSDRNPM results discussed in the optimization analysis. Based on the results of Table 5 the ruptured knockout canister was used in subsequent analysis of the transfer shield and cask. (2)

Table 5. Canister - Transfer Shield Optimization Results

| | K-effective/2σ | Keno Bias | Max. K-effective | Neutron Histories | |
|---|---|---|---|---|---|
| Transfer Shield** w/Knockout Canister | .887±.009 | .02 | .916 | 21371 | (1) |
| Transfer Shield** w/Filter Canister | .851±.011 | .02 | .882 | 18361 | (1) |
| Single Knockout* Canister, No Shield | .844±.016 | .02 | .880 | 10234 | (1) |
| Single Filter Canister,* No Shield | .806±.014 | .02 | .840 | 9331 | (1) |

*From Reference 2.
**These cases were run for a canister shield gap of 0.5 inches.

## 3.13. Canister Insertion Analysis

### 3.13.1. Model Description and Background

From the canister optimization study it was determined that the knockout canister was the most reactive canister type. For that analysis it was assumed, based on XSDRNPM results, that a canister fully inserted into the transfer shield was the most reactive configuration. This assumption is verified by the insertion study described in this section.

The basic transfer shield model is the same as that described in the canister optimization study. To simplify the generalized geometry, the canister will be raised into the shield with the water level flush with the bottom of the shield to prevent neutron streaming. The outer shield will not be extended below the water surface since XSDRNPM results from the gap study indicated that lead with an air gap is more reactive than lead with a water gap by approximately 1.9%Δρ. The horizontal six inch lead shield will be maintained 20 inches above the canister upper head even though the downward travel of this shield is limited to the lower end of the inner shield. This approximation is conservative for the smaller percentage insertion cases because the 6 inch horizontal shield will be modeled closer to the upper head than it should be maximizing K-effective. (2)

Figure 6 shows the knockout canister at its 6.8, 54.4, 96.6, and 100% insertion levels. These levels correspond to the different geometry block boundaries. Other insertion levels were used to generate the insertion curve shown in Figure 7. Although the problem "snapshot" changes in Figure 6 as the knockout canister is inserted into the shield the area being modeled is sufficiently large that material effects external to the problem boundary are insignificant in the computation of K-effective. This is true in the water moderated region where a minimum of 12 inches of water is used, effectively

decoupling the canister from other pool materials. Neutrons that do penetrate the lead shield above the water surface stream through the air medium and would probably not return to the canister-shield system. Effects of the pool walls and other concrete structures were not considered since pool-wall reflector calculations in references 2 and 3 demonstrate that concrete behaves in a fashion similar to water. The effect of the concrete will be to thermalize most neutrons escaping from the lead shield. For those concrete reflected neutrons that have traversed the lead shield, they would be subject to absorption in the steel canister shell and gap medium prior to reaching the fuel water mixture. Finally, the water reflector analysis of section 3.10 (2) demonstrated that if the entire transfer device were surrounded by water, the most K-effective could increase from reduced leakage is .0081 Δk. Since it is not possible to completely surround the shield with concrete, any increase in K-effective from walls or other structures will be small. For these reasons it is felt that an external concrete structure near the transfer shield or cask will have a negligible impact on the calculated K-effective.

### 3.13.2. Canister Insertion Analysis Results

The results of the transfer shield insertion study with the knockout canister are tabulated in Table 6 and shown in Figure 7. These results confirm the XSDRNPM results that the most reactive configuration is for the knockout canister fully inserted. The cases performed for the revision 1 insertion study used the knockout canister model that does not reflect the recent 3.75 inch reduction in the four outer $B_4C$ poison rods. The 3.75 inch reduction in length represents only a 2.8% reduction in the total poison length and should not result in a more significantly limiting insertion case.

Figure 6

Typical Ruptured Knockout Canister
Insertion Levels in Transfer Shield

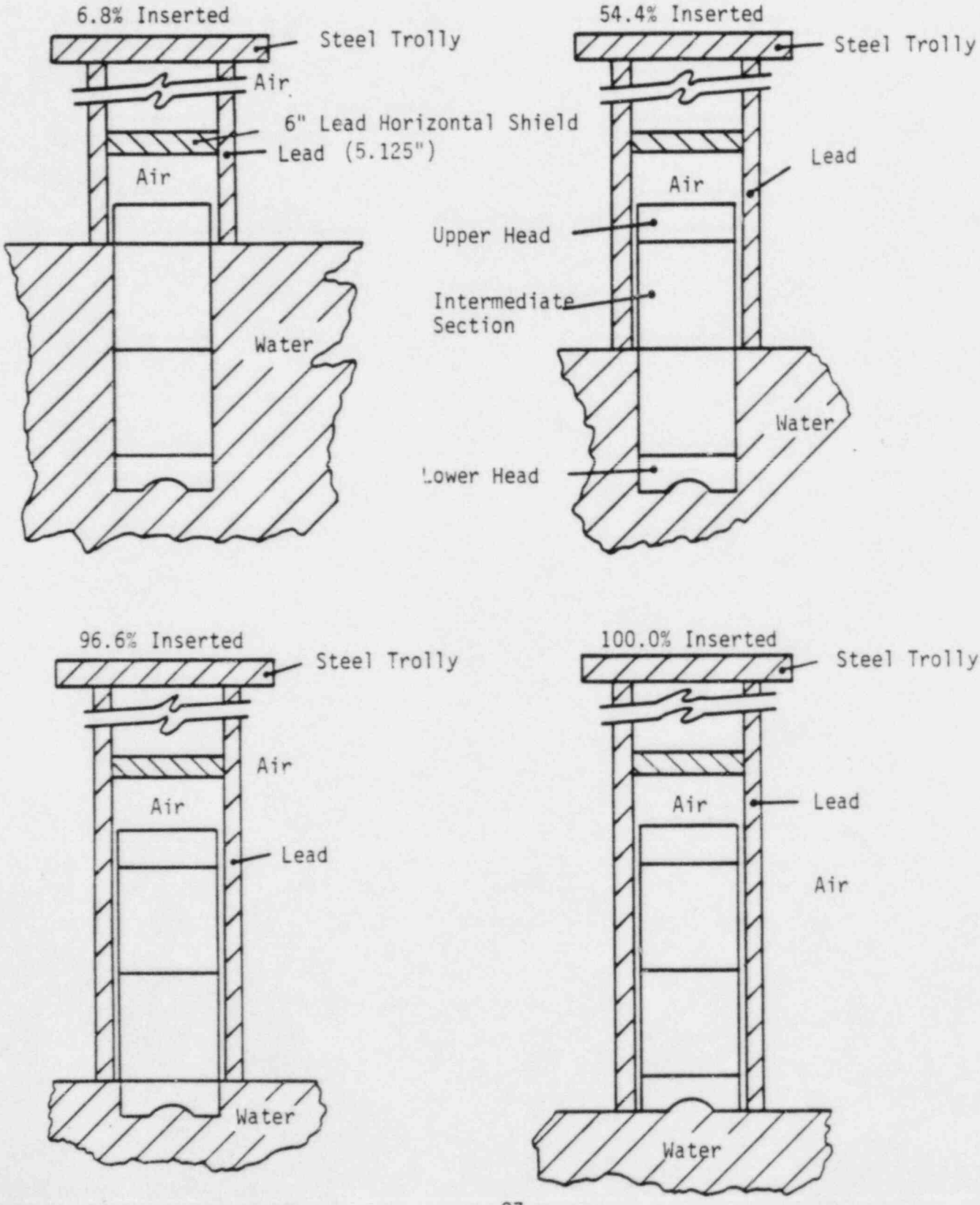

This effect was verified by computing the ruptured knockout canister case fully inserted into the transfer shield with the shortened rods. The resultant K-effective was .002 smaller than the case with longer rods and is shown in Table 6. This difference in K-effective is insignificant since it is smaller than the .006-.007 2σ KENOIV uncertainty. Because of the insignificance of the $B_4C$ rod length change on K-effective values, the original studies are valid for the current design. Since the transfer cask is similar to the transfer shield, the fully inserted position should be optimum for the cask, especially with the cask lead door closed.

Also included in Table 6 is a reanalysis of the ruptured knockout canister 100% inserted into the transfer shield. The transfer shield was modeled according to dimensions in Figure 2. Differences between this calculation and earlier analysis are: (2)

1) The exact height of the outer 9 foot and 30 inch shields are modeled.
2) The water reflector outside of the shield is raised 2 feet.
3) The new knockout canister geometry with baffle plate modifications and poison rod length reductions are implemented.
4) The steel liners are modeled in the shield walls.

With the above modifications, the resultant K-effective is 0.879 ± .01 which yields a maximum K-effective with the KENOIV bias of .909. These results are consistent with the revision 1 analysis indicating the earlier cases are sufficiently conservative.

Two additional cases were calculated for the transfer shield. The first case utilized the NULIF code to determine an optimum fuel-water volume fraction with low density water. An optimum fuel volume fraction of 0.021 was determined for 0.05 g/cc dense water. This case was performed because of a concern that for low density water cases there could exist the possibility of

a secondary reactivity spike for an array of assemblies or canisters. Since lead and steel are good reflectors of neutrons this case was performed to ensure that neither the transfer shield or cask could imitate this array effect. As Table 6 indicates, K-effective is nearly zero due to the low fission density of neutrons. This low fission density is the result of the small optimized fuel volume at low water densities together with significant amounts of structural and poison material. The second case also utilizes 0.05 g/cc dense water but for a fuel-water volume fraction of .31084. As shown in Table 6, this case yields a maximum K-effective of only .205. Therefore, it appears that the reactivity spike at low water densities does not occur for single canisters in a lead shielded device. (2)

Table 6. Knockout Canister Insertion Study
K-effective Results

| % Inserted | K-effective/2σ | KENO Bias | Max K-effective | Neutron Histories | |
|---|---|---|---|---|---|
| 100.0% | .882±.006 | .02 | .908 | 38354 | (1) |
| 86.0% | .881±.007 | .02 | .908 | 39864 | (1) |
| 65.0% | .875±.007 | .02 | .902 | 37448 | (1) |
| 54.4% | .866±.008 | .02 | .894 | 30200 | (1) |
| 42.4% | .855±.009 | .02 | .884 | 21744 | (1) |
| 22.8% | .836±.011 | .02 | .867 | 16610 | (1) |
| 6.8% | .827±.011 | .02 | .858 | 19328 | (1) |
| 100.0% (short rods) | .880±.007 | .02 | .907 | 42582 | (1) |
| 100.0% (new canister and shield geometry) | .879±.010 | .02 | .909 | 23655 | (2) |
| Optimized Fuel (.021 VF fuel, 0.05 g/cc dense water) | .020±.001 | .02 | .041 | 16185 | (2) |
| Low Water Density (.31084 VF fuel, 0.05 g/cc dense water) | .181±.004 | .02 | .205 | 16600 | (2) |

Examination of the scattering cross-section for iron in the epithermal range indicates that steel in air could be potentially as good of a reflector of epithermal neutrons as lead due to both cross-section magnitude and the higher number density of iron atoms. To investigate the significance of steel versus lead in an air medium, three XSDRNPM cases were performed with cylindrical geometry. The cases performed consisted of a shield containing a thickness of 8.5 inches of lead, one containing 8.5 inches of steel, and one with 8.5 inches of alternating layers of steel and lead according to Figure 3. (2)

Figure 7

Reactivity Dependence of Knockout Canister
Insertion Into Transfer Shield

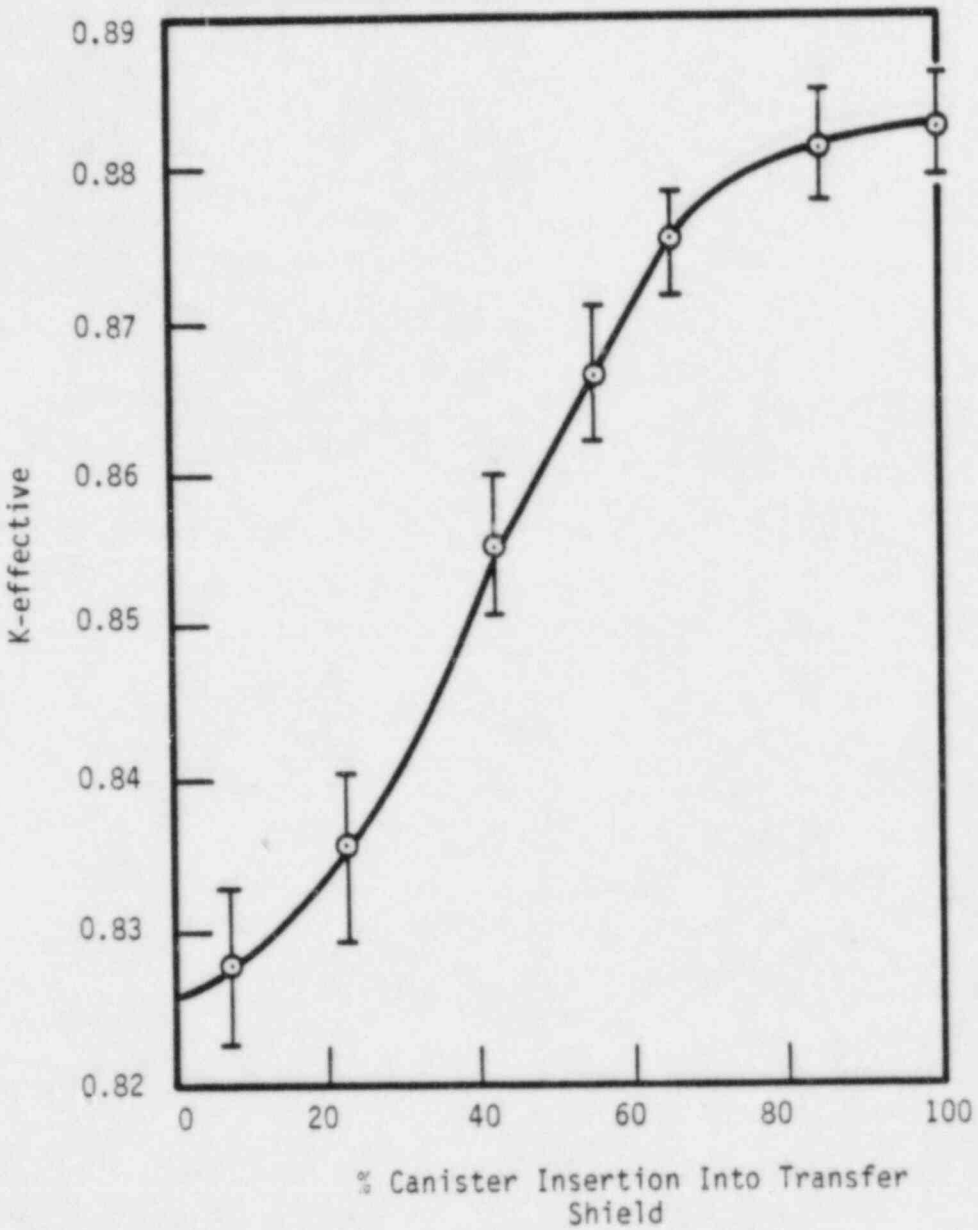

From the XSDRNPM results shown in Table 7, the all steel shield is more reactive than the all lead shield case by .004 Δk.

However, when steel and lead are combined there is a decrease in K-effective relative to the all lead case of .002 Δk. This decrease in K-effective is currently thought to be a space-energy interaction between the steel and lead. Since both the transfer shield and cask have alternating layers of steel and lead, the steel liners in all revision 2 analyses are modeled. (2)

Table 7. XSDRNPM Steel Liner Analysis*

| Cell Type | Model | K-Effective | |
|---|---|---|---|
| 14 inch canister, air gap, 8.5" steel shield | XSDRNPM | 1.03371 | (2) |
| 14 inch canister, air gap, 8.5" lead shield | XSDRNPM | 1.02961 | (2) |
| 14 inch canister, air gap, 8.5" shield with alternating layers of steel and lead | XSDRNPM | 1.02742 | (2) |

*The absolute magnitude of k-effective is not significant. Cell results used to indicate trends.

## 3.14. Transfer Cask Analysis

### 3.14.1. Model Description and Background

The transfer cask is shown in figure 4. The 15 foot 1 inch long upper lead shield is 4.5 inches thick with an additional 1 inch steel liner on both sides. A 6 inch thick horizontal lead shield, located 10 inches above the upper head of the knockout can is assumed. The bottom lead door, shown in the closed position in Figure 4, is 4 inches thick with an additional 0.5 inch of steel liner on all sides. For revision 2 analysis only, the region below the 4 inch lead door was filled with lead to add an extra 5 inches of lead for conservatism. This gives a combined lead and steel thickness below the canister of 10 inches. It is assumed the door consists of two hemi-cylinders that can be opened. For conservatism in revision 2 calculations only, the (2)

door was extended to an outside diameter of 43 inches and is indicated in Figure 4. Located below the bottom door is a lead shield flange that projects 7.5 inches in a radial direction beyond the main cask walls. This lead flange is also 4 inches thick with an additional 0.5 inch thick steel liner on all sides. The total length of the flange is 14 inches. A lower shield collar, called a loading boot was included in the model and extends 2 feet into the pool. The loading boot has a 3 inch lead thickness with a 1 inch steel liner on all sides. The total length of this collar is assumed to be 3 feet. Although the loading boot is no longer required, it was maintained for conservatism since the inside diameter of the loading boot is less than the optional vertical shield used with the cask. The inside diameter of the transfer cask is assumed to be 15 inches resulting in a 0.5 inch air gap between the canister and the inner cask wall steel liner. (2) (2)

3.14.2. Cask Analysis Results

Since it was determined from the transfer shield insertion study that the fully inserted canister is most reactive, calculations using the ruptured knockout canister were performed with the canister fully inserted and the bottom lead door closed. Results from the ruptured knockout canister fully inserted into the transfer cask are shown in Table 8. These results indicate that with the 2$\sigma$ uncertainty and KENOIV bias added, the maximum K-effective is less than the .95 criteria. This calculation was performed for the ruptured knockout canister with the original longer $B_4C$ rods. The previous insertion study demonstrated that the reduction in poison length by 3.75 inches resulted in an effect on K-effective of less than the 2$\sigma$ uncertainty of the calculation.

It was not expected that the external lead/steel flange would have any significant impact on the worst reactive insertion position since this flange

is 10 inches thick and would cover only a 2.8% slice of the canister at any time during insertion. To verify this assumption and to simplify geometry modifications, early calculations were performed with an additional 10 inch thick lead/steel collar, 7.5 inches thick radially, that was added to the outside of the cask at the approximate midplane of the knockout canister. This position will be nearly the most reactive position for this canister design. Additionally, the outer $B_4C$ rods were 3.75 inches shorter. This case in all other respects is the same as the previous case with longer rods. Since both the additional lead and shorter $B_4C$ rods are positive reactivity additions, the close reactivity agreement between the first and second cases indicates that the change in poison rod length and additional lead collar have an insignificant effect on reactivity. These conclusions are in close agreement with the transfer shield insertion study which also indicated the difference in $B_4C$ length to be within the KENOIV uncertainty.

One additional cask case was run which utilized the exact geometry of the knockout canister with the revised baffle plate positions and poison rod lengths. In addition, extra lead was added below the bottom door and in the flange region for conservatism. This case shown in Table 8 is the most limiting of all cases examined with a maximum k-effective of .931. (2)

The results of the insertion analysis for the ruptured knockout canister in the transfer cask indicate that criticality criteria will not be violated. It is therefore reasonable to assume that no borated polyethylene liner will be required as a reactivity control device for either the transfer shield or cask. No analysis has been made of externally damaged or deformed canisters since these canisters will be handled by GPUN on a case by case basis and therefore are not included in the current workscope. (2)

Table 8. K-effective for the Ruptured Knockout Canister in the Transfer Cask

| % Inserted | K-effective/2σ | KENO Bias | Max. K-eff | Neutron Histories | |
|---|---|---|---|---|---|
| 100% (Longer $B_4C$ rods) | .897±.006 | .02 | .923 | 47725 | (1) |
| 100% (Shorter $B_4C$ rods and extra lead collar) | .897±.007 | .02 | .924 | 43990 | (1) |
| 100% (Latest geometry and extra lead) | .904±.007 | .02 | .931 | 40255 | (2) |

## 4. Conclusions

With the canister design assumptions defined by references 2 and 3 and unique cross-section sets generated by the NITAWL-XSDRNPM codes, the optimal fuel volume mixture was demonstrated to remain as .31084 with a 6 inch lead shield. Conditions of water at 50°F and 100% nominal density were demonstrated to be most reactive.

The most reactive compositions for the gap region between the canister and transfer cask or shield lead wall was shown to be either void or air. Partial mixtures of water and air and pure water were shown to be less reactive compositions for the gap region. Water regions surrounding the lead shield were shown to be small positive reactivity additions and less than the gap effect. XSDRNPM slab calculations demonstrated that there was almost no change in K-effective for an off-centered canister within the transfer shield with the centered position being most reactive. (2)

Insertion studies with the transfer shield demonstrate that the knockout canister is the most reactive of the three canister designs. The presence of a transfer shield provides a reactivity increase over the single canister in water of approximately (.055 to .06$\Delta$k) $\pm$ .018$\Delta$k. The insertion analyses also defined the 100% insertion level as the most reactive configuration for a canister in either the transfer shield or cask. Modeling the steel liners within the transfer shield wall as well as other modeling changes resulted in K-effective being nearly the same as that computed by earlier shield models. Therefore, previous analyses for the transfer shield are sufficiently conservative. XSDRNPM calculations verified that an all steel liner is more reactive than an all lead liner by 0.004 $\Delta$k. A combined steel and lead liner was found to be 0.002 $\Delta$k less reactive than the all lead shield. Further analyses for the transfer shield with a reduced water density of 0.05 g/cc verified (2)

that there is no secondary reactivity spike for low water density cases. Analyses were performed for the knockout canister in the transfer shield and cask with the 3.75 inch shortened outer $B_4C$ rod modification. These results demonstrated that the reactivity increase due to the slightly shorter outer $B_4C$ rods is less than the KENOIV uncertainty. The effect of the lead/steel flange was conservatively quantified by placing an additional lead collar around the middle of the transfer cask at potentially the most reactive position with a knockout canister fully inserted. Since the collar could cover only 2.8% of the canister at any time during insertion, the reactivity effect was shown to be less than the KENOIV uncertainty and calculationally insignificant. A cask case was performed implementing the latest knockout canister geometry which exactly models the shorter poison rods and the revised baffle plate locations. Extra lead was added to the bottom door and flange region of the cask for conservatism. This case was the most limiting with a maximum K-effective of 0.931. (2)

Results of these analyses indicate that no borated polyethylene or other poison material is required in the design of the transfer shield or cask for reactivity control. These results are valid for standard unruptured canisters and canisters with internally ruptured filter screens containing fuel in upper and lower head regions. Canisters with extensive internal damage and/or external damage from being dropped and deformed are not addressed since these canisters will be handled by GPUN on a case by case basis and therefore are not included in the current workscope. (2)

## 5. References


1. "Canister Transfer System Information," 38-1013198-00, Dec. 4, 1984.

2. "TMI-2 Defueling Canisters Final Design Technical Report," Document 77-1153937-00 (B&W), October 31, 1984.

3. "TMI-2 Defueling Canisters Final Design Technical Report," Document 77-1153937-04 (B&W), May 1985. (2)

4. "Technical Specification for Design of Defueling Canisters for GPU Nuclear Corporation Three-Mile Island - Unit 2 Nuclear Power Plant," 53-1021122-01 (B&W), Rev. 2, July 17, 1984.

5. "Licensing Requirements for the Storage of Spent Fuel in an Independent Spent Fuel Storage Installation," 10CFR72, U.S. Nuclear Regulatory Commission, Rev. 1, May 1977.

6. "Nuclear Criticality Safety in Operations with Fissionable Materials Outside Reactors," American National Standards Institute, American National Standard, ANSI/ANS 8.1, 1983. (2)

7. "Criticality Safety Criteria for the Handling, Storage, and Transportation of LWR Fuel Outside Reactors," American National Standards Institute/ American National Standard, ANSI/ANS 8.17, 1984.

## 5. References (cont'd.)


8. "Guide for Criticality Safety in Storage of Fissionable Materials," American National Standard, ANS 8.7/N16.5, 1982. (2)

9. "NULIF - Neutron Spectrum Generator, Few Group Constant Calculator and Fuel Depletion Code," BAW-426, Rev. 5, January 1983.

10. "NITAWL Nordheim Integral Treatment and Working Library Production," (B&W Version of ORNL Code - NITAWL), NPGD-TM-505, Rev. 5, June 1984.

11. "XSDRNPM AMPX Module with One-Dimensional Sn Capability for Spatial Weighting," AMPX-II, RSIC-RSP-63, ORNL.

12. "KENO4, An Improved Monte Carlo Criticality Program," (B&W Version of ORNL Code, KENOIV), NPGD-TM-503, Rev. B, August 1982.

13. W. R. Cable, "123 Group Neutron Cross Section Data Generated From ENDF/B-II Data for Use in the XSDRN Discrete Ordinates Spectral Arraying Code," RSIC-DLC-15, ORNL, 1971.

14. M.N. Baldwin, et.al., "Critical Experiments Supporting Close Proximity Water Storage of Power Reactor Fuel," BAW-1484-7, July 1979, (B&W) (available from National Technical Information Service), Rev. 0.

## 5. References (cont'd.)

15. F.M. Alcorn, "Nuclear Criticality Safety Benchmark Notebook," Rev. 2, February, 1984. (LRC document)

Attachment 2

Assessment of a Drained Pool Scenario

# TMI-2 Drained Pool Analysis

## Cases Analyzed

Two drained pool cases representing different states of internal canister moderation are considered here. These cases are judged to be bounding with respect to the possible real contents of the canisters in the unlikely event of loss of pool water. The conditions assumed for these cases are as follows:

Case 1: Optimal fuel volume fraction in 4350 PPM boron moderator of full density at 50°F.

Case 2: Realistic fuel volume fraction with pure water moderation at 100% humidity conditions at 50°F.

## Calculational Models and Procedures

In both cases the basic canister model is the standard configuration knock-out canister described in B&W Document No. 77-1153937-03, page 2-31. For conservatism, and to facilitate modeling in KENO standard geometry, the four satelite poison tubes and all lateral support plates are omitted and their space is occupied by fuel.

Additional conservatism is provided by assumptions of infinite extent of the canister array and enhancement of overhead reflection by concrete modeled above the array. A 17.3 inch square pitch was assumed.

For Case 1, the optimal fuel volume fraction was determined by NULIF calculations to be 0.620 with a $K_\infty$ of 1.02890 and cell weighted cross sections for the KENO calculations were generated by NITAWL/XSDRNPM calculations.

For Case 2, a measured fuel volume fraction for randomly packed whole fuel pellets was used (B&W Commercial Plant License SNM-1168, Docket 70-1201, Section 3, page 35). THis volume fraction was 0.624 which by coincidence is close to that of Case 1. NULIF calculation for this volume fraction with saturated steam (pure $H_2O$) as moderator gave a $K_\infty$ of 0.65706. Further NULIF calculations at this fuel volume fraction vs. increasing water density gave a monotomically increasing $K_\infty$ up to 1.21412, at 100% water density. However, beyond the saturation point there would be liquid water not removed in the dewatering process and this water would be borated. This condition is covered in Case 1.

## Results and Conclusions

For Case 1, the calculated maximum $K_{eff}$, including a 0.02 benchmark uncertainty and the 2-sigma KENO uncertainty, is 0.964. This is for an infinite X-Y array with no concrete side reflection. The effect of concrete reflection on the sides rather than an additional knockout canisters was shown to be negative with respect to reactivity.

For Case 2, the very low value of $K_\infty$ compared to that for Case 1 assures that $K_{eff}$ for an array of canister will be well below that for Case 1. This was verified by a KENO calculation for an infinite 17.3 inch pitch array yielding a value of $K_{eff}$ of 0.532 including uncertainties. The effect of concrete reflection was found to be negative for this case also.

It is concluded that no realistically conceivable conditions that could occur during a TMI-2 storage pool drainage event would lead to a value of $K_{eff}$ greater than the specified 0.99 acceptance criterion. This assumes that diluting or reflooding the canister contents with pure water is precluded by administrative control.